Rigorous Evaluation of Liquid Products at High-rate CO_2/CO Electrolysis

Ming Ma,*[,†] Zhe Zheng,[†] Wen Yan,[†] Chao Hu[†] and Brian Seger*[,§]

[†]School of Chemical Engineering and Technology, Xi'an Jiaotong University, Xi'an 710049, People's Republic of China
[§]Department of Physics, Technical University of Denmark, 2800 Kgs. Lyngby, Denmark

ABSTRACT: In this work, the water crossover in CO_2 electrolysis was systematically analyzed with hydrated ions transferring through ion-selective membranes as charge carriers in three-compartment devices. We demonstrate that the water crossover leads to a variation in the electrolyte volume, which plays an important role in the evaluation of the catalytic selectivity of liquid products. Without considering the water crossover, the catalytic selectivity of liquid products could be overestimated with the use of anion exchange membranes and underestimated with cation exchange membranes. In addition, a protocol for reliably quantifying liquid product is proposed for high-rate CO_2/CO electrolysis in three-compartment flow electrolyzers.

The electrocatalytic conversion of CO_2 represents an emerging and promising technology in the production of carbon-neutral fuels and chemicals using renewable electricity.[1–6] In the past decade, fundamental understanding of CO_2 electrolysis technology and the development of high-performance catalysts have been intensively explored at low current densities (j) using traditional H-cell devices.[7–10] For achieving practical utilization of CO_2 with high conversion rates, CO_2 electrolysis technology in recent years has progressed from H-cells that only allow for low reaction rates (i.e. low j) to flow-electrolysers with gas diffusion electrodes (GDEs) operating at high reaction rates (*i.e.* j > 100 mA/cm^2).[11–15] However, operation at commercially relevant current densities inevitably adds complexities in the evaluation of the catalytic performance, particularly in terms of the catalytic selectivity.

The reliable quantification of gaseous CO_2 reduction products mainly relies on the accuracy of the detected concentration and the related gas flowrates. However, in high-rate CO_2 reduction, most of the consumed CO_2 reacts with OH^- near the cathodic GDE/electrolyte interface, forming carbonate, and this consumption of CO_2 can lead to a considerable decrease in gas outlet flowrates.[16] Without considering the variation in gas outlet flow (*i.e.* the CO_2 consumption), the faradaic efficiency (FE) of gas products can be significantly overestimated, especially when using highly concentrated alkaline electrolytes.[16] Thus, flow out of electrolyzers needs to be monitored for accurately evaluating catalytic selectivity (*i.e.* FE) of gas products. After realizing this issue, some recent works started to explicitly state that their faradaic efficiency calculations were based on the outlet gas flow.[12,17–20]

In addition to gaseous products, the liquid products of CO_2/CO reduction are generally quantified by measuring a concentration (e.g. via a HPLC) and related solution volume, according to the faradaic efficiency (FE) calculation of liquid products as follows:

$$FE\ (\%) = \frac{nC_{liquid\ product}VF}{Q_{tot}} \times 100\% \qquad (1)$$

where n is the number of electrons required for forming one molecule of the corresponding liquid product. $C_{liquid\ product}$ and V are the molar concentration of liquid product and the volume of the electrolyte, respectively. F is Faraday constant, and Q_{tot} is the total charge passed through the working electrode.

It has been demonstrated that the quantification of liquid products requires the analysis of both catholyte and anolyte as well as liquid products evaporated from GDEs into the gas chamber of flow-electrolysers.[21,22] It should be noted that when ionic species transport via ion-selective membranes as charge-carriers during electrolysis, water molecules also cross over via the membrane through electro-osmotic drag as hydrated ions (i.e. ions carrying with water molecules) migrate. At low current densities (such as most of studies in H-cell) with short-term (several hours) electrolysis, water crossover via membrane can be negligible since the total charge transferred across the membrane is very low (*i.e.* very small amounts of ion transfer). Thereby, it is reasonable to calculate faradaic efficiency of liquid products via a detected concentration and corresponding volume that is relatively approximated by the initial volume of the catholyte or anolyte. However, for high current density CO_2/CO electrolysis, substantial amounts of ions transferred via membranes may lead to considerable water crossover via the membranes in reactor designs with flowing-catholyte, which can significantly change the catholyte and anolyte volume. Thus, the measurement of the electrolyte volume (particular for the catholyte volume) after high-rate electrolysis plays a crucial role in the faradaic efficiency calculation of liquid products. However, most of high-rate CO_2/CO reduction studies have not explicitly stated that their faradaic efficiency calculations of liquid products were determined by the volume of electrolyte after electrolysis. If their assessment of their liquid product selectivity and activity was based on the initial electrolyte volume, their results may be inadvertently distorted. Thereby, to prevent results from being errantly reported in GDEs-type electrolyzers, it is essential to systematically explore the water crossover via membranes and benchmark the evaluation of the catalytic selectivity for liquid products at high current densities.

Herein, we experimentally demonstrate that water crossover through ion-selective membranes can significantly vary the volume of catholyte and anolyte in a three-compartment flow-electrolyzer, especially when ionic species with high hydration number are used as charge-carriers for an anion exchange membrane (AEM) or cation exchange membrane (CEM). By a systematic exploration of water crossover rate and the molecular ratio of water/charge-carrying ion crossed through the membranes, this study shows how charge-carrying ions and their surrounding water molecules affect the evaluation of catalytic selectivity for liquid products at high-rate CO_2/CO electrolysis. In addition, this study also provides a rigorous protocol for the quantification of liquid products, which enables us to get more accurate results for high-rate CO_2/CO electrolysis.

All the CO_2 or CO electrolysis experiments were performed in a Teflon flow-electrolyzer consisting of gas, catholyte and anolyte compartments, as presented in Figure 1. In this custom-made three-

compartment electrolyzer, a Cu layer prepared on microporous layer of GDE by magnetron sputtering was positioned between the gas and catholyte compartments. The GDE cathode with a geometric active area of 2 cm^2 was utilized in all the experiments. In addition, the catholyte and anolyte compartments were separated by an ion-selective membrane (Figure 1) that allows hydrated ions to transport as charge-carriers. For systematically exploring the water crossover issue, anion exchange membranes (Fumasep FAA-3-PK-75), cation exchange membranes (Nafion™ 212) and bipolar membranes (BPMs, Fumasep FBM) were all utilized in this study, respectively.

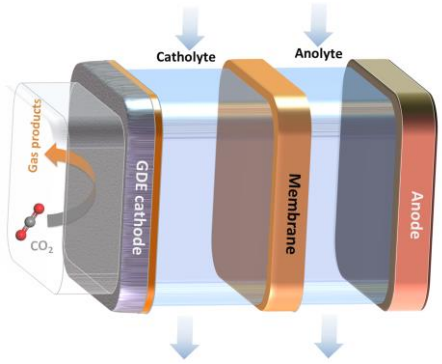

Figure 1. Schematic illustration of three-compartment flow electrolyzer that encompasses gas, catholyte and anolyte compartments.

Water crossover for an AEM

In most of the high-rate CO_2/CO reduction research to date, anion exchange membranes have been employed to separate catholyte and anolyte chambers in GDE-type flow-electrolyzers (Figure 1). In addition, highly concentrated $KHCO_3$ or KOH electrolyte is widely used in flow-electrolyzers, which means that HCO_3^- or OH^- is the dominant ion transferring across the AEM, respectively, assuming no ionic species change in the catholyte. Thus, to uncover the water crossover issue via an AEM in flowing-catholyte electrolyzers, the electrolysis experiments in this work were performed via the typical anion species of HCO_3^-, OH^-, and CO_3^{2-}, respectively.

Specifically, to ensure HCO_3^- as domination anion transferring via the AEM, CO_2 electrolysis was performed in 1 M $KHCO_3$, which was continuously bubbled with CO_2 in the catholyte reservoir during electrolysis (Figure S1). The catholyte pH was also monitored during CO_2 electrolysis. We found that pH value in the catholyte was maintained below ~8.8 over 5 h electrolysis (Figure S4), which reveals that the concentration ratio of CO_3^{2-} to HCO_3^- was below ~0.04 based on the Henderson–Hasselbalch equation (Equation S1). This finding indicates that HCO_3^- should serve as the dominant charge-carrying species transferring from catholyte to anolyte via the AEM over the entire electrolysis experiment when using CO_2-bubbled 1 M $KHCO_3$. In addition, it has been demonstrated that the catholyte change from HCO_3^- to CO_3^{2-} at high-rate CO_2 reduction in our previous work,[16] thereby CO_2 electrolysis was directly carried out in 0.5 M K_2CO_3 catholyte (Figure S2), which can easily keep CO_3^{2-} as the major charge-carriers via the AEM. Furthermore, to maintain OH^- as the dominant anion transferring via the AEM, Ar/CO instead of CO_2 was fed into the gas compartment for electrolysis in 1 M KOH (Figure S3). To avoid the anionic liquid products effect, Ar was fed into gas chamber. The constant pH in catholyte was observed over the electrolysis in 1 M KOH (Figure S5), owing to that the supply rate of OH^- via cathodic reactions should equal the transport rate of OH^- via the AEM, thus confirming that OH^- is the dominant ion being transported. All these experiments enable us to explore the water crossover via the AEM when transferring HCO_3^-, OH^-, and CO_3^{2-}, respectively.

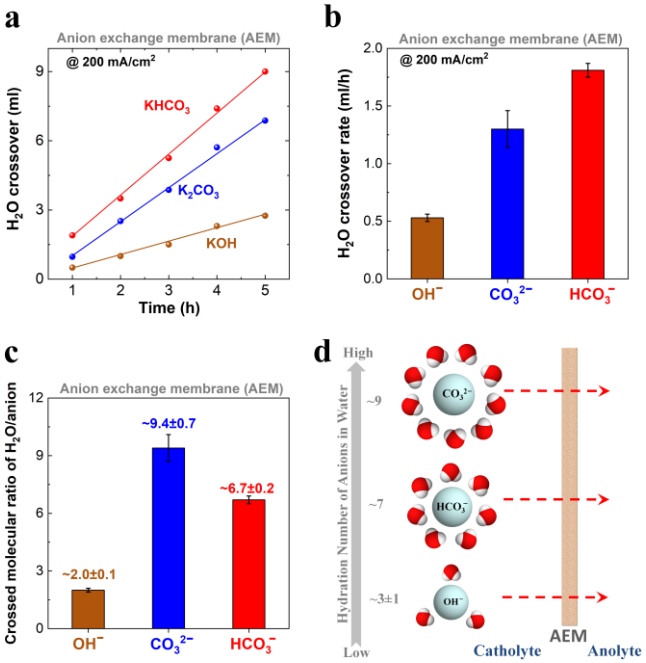

Figure 2. Comparison of water crossover from catholyte to anolyte via an AEM when transporting different anions. (a) Water volume transferred from catholyte to anolyte over electrolysis. (b) Estimated water crossover rate (*i.e.* water flux via the AEM) and (c) corresponding molecular ratio of water/anion crossed through the AEM. (d) Schematic illustration of hydrated anions crossover through the AEM. Distinct anions species hydrated with different numbers of water molecules. The red and white balls represent O and H atoms, respectively.

A comparison of water crossover volume over the course of electrolysis with different anion species transferring across the AEM is presented in Figure 2a. As the electrolysis time increased, water crossover volume from the catholyte to anolyte gradually enhanced when transferring the three different anions, respectively (Figure 2a). Notably, a considerable water crossover of more than 9 ml was observed after 5 h electrolysis when using HCO_3^- as the charge-carrier via the AEM. In contrast, a small amount of water crossover (only ~3 ml) occurred for only transferring OH^- via the AEM. The above discrepancy in total volume of water crossover reveals the distinct water transport rate (Φ) toward anolyte with transferring different anion species (*i.e.* decrease rate of catholyte volume: $HCO_3^- > CO_3^{2-} > OH^-$), as shown in Figure 2b.

In addition, it should be noted that the decrease rate in the catholyte volume (Figure S6b) was slightly larger than the water transport rate (Figure 2b). This observation is primarily due to that the cathodic reactions (Equation S3-S9) consume water, and this water consumption rate depends on catalytic selectivity (Equation S10). For instance, when transferring HCO_3^-, the theoretically calculated water consumption rate via the cathodic reactions was ~0.17 ml/h (Table S1), adding with the measured water crossover rate (~1.81 ml/h in Figure 2b) to get a total water consumption rate of 1.98 ml/h in the catholyte, which is almost equal to the measured decrease rate in the catholyte volume (Figure S6b).

To better understand water crossover with different ions, the molecular ratio of H_2O/anion crossed through the AEM was calculated based on equation S11. As noted in Figure 2c, the average number of water molecules of ~2.0, ~9.4 and ~6.7 was found when transferring each OH^-, CO_3^{2-} and HCO_3^-, respectively, which is relatively consistent with the previously reported hydration number of hydroxide,[23] carbonate[24,25] and bicarbonate[25]. Thus, the discrepancy in water crossover rate for different anionic species is linked

to their hydration numbers (Figure 2d). As a substantial amount of CO_3^{2-} or HCO_3^- was transferred at high-rate electrolysis, its large hydration number (Figure 2d) could lead to a considerable water crossover from catholyte to anolyte via the AEM at flowing-catholyte devices (Figure 2a), thus significantly reducing catholyte volume while increasing anolyte volume. In addition, it should be noted that while hydration number of HCO_3^- is lower than that of CO_3^{2-} (Figure 2d), hydration number/charge ratio for HCO_3^- is larger in comparison with that of CO_3^{2-}, corresponding to a larger amount of water crossover when transferring HCO_3^- via the AEM under identical conditions.

Water crossover for a CEM

While only a few studies on high-rate CO_2 electrolysis have been performed using CEM,[26–28] we have demonstrated that the utilization of CEM is capable of circumventing the CO_2 crossover from catholyte to anolyte.[22] Recently, the Sargent group reported that high-rate CO_2 reduction in acidic electrolytes with the use of CEM could significantly enhance the CO_2 utilization rate.[12] Since a CEM approach could circumvent CO_2 crossover and have great potential for increasing CO_2 utilization rate, we herein explored the water crossover issue via a CEM at flowing-catholyte electrolyzers using the typical cation species of Li^+, K^+, and Cs^+, respectively.

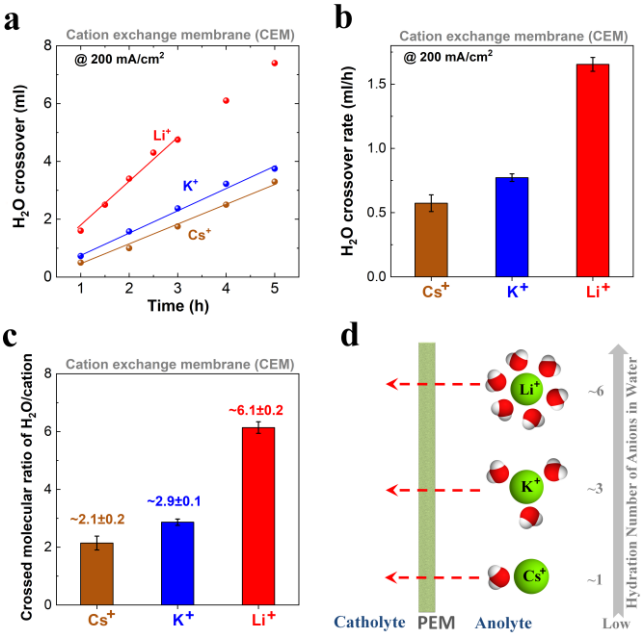

Figure 3. Comparison of water crossover from anolyte to catholyte via a CEM when transporting different cations. (a) Water volume crossed from anolyte to catholyte over electrolysis (Li^+ data within the initial 3 h was used). (b) Estimated water crossover rate (*i.e.* water flux via the CEM) and (c) corresponding molecular ratio of water/cation crossed through the CEM. (d) Schematic illustration of hydrated cations crossover through the CEM. Distinct cations species hydrated with different numbers of water molecules. The red and white balls represent O and H atoms, respectively.

To ensure the aforementioned cation species act as the dominant species transferring through the CEM, buffered electrolytes need to be employed in CO_2 electrolysis. Without using buffering electrolytes, the significant amount of H^+ generated via O_2 evolution reaction (equation S12) at high current densities may lead to an acidification of anolyte. This anolyte acidification could lead to a corresponding changing of the main transport charge-carrier for CEM from metallic cation species to H^+ over the electrolysis. Therefore, in this study, 2 M K_2CO_3 and 2 M Cs_2CO_3 were utilized for exploring water crossover issue when transferring K^+ and Cs^+, respectively. The use of electrolyte containing CO_3^{2-} can neutralize H^+ produced at the anode/electrolyte interface, releasing gaseous CO_2 along with O_2 while avoiding an acidification of the anolyte. Due to that Li_2CO_3 has a very low solubility, 2 M Li_2SO_4 was used for the investigation of the water crossover issue with Li^+. If we assume that the produced H^+ is collected in the anolyte (50 ml) over 3 h electrolysis at 200 mA/cm^2, the concentration of H^+ would be ~ 0.9 M (Table S2), which is much lower than that (4 M) of Li^+. In addition, Li^+ is more preferable to cross over the CEM when mixing with H^+.[²⁹] Thus, while Li_2SO_4 electrolyte is unable to buffer the produced H^+ at the anode/electrolyte interface, the dominant cation transferring across a CEM should be Li^+ within 3 h electrolysis. Based on these experiments, we studied the water crossover via the CEM when transferring Li^+, K^+, and Cs^+, respectively (Li^+ data within the initial 3 h electrolysis was used).

Figure 3a shows a comparison of water crossover volume over the course of electrolysis with transferring Li^+, K^+, and Cs^+ via the CEM, respectively. We found a linear relationship between the water crossover volume and electrolysis time when the same kind of cation was transferred via the CEM (Figure 3a). In addition, the difference in total volume of water crossover after 5 h electrolysis corresponds to the discrepancy in the water transport rate from the anolyte to the catholyte (Figure 3b) (*i.e.* increase rate of catholyte volume: $Li^+ > K^+ > Cs^+$). As noted in Figure 3c, the molecular ratios of H_2O/cation crossed through the CEM were ~2.1, ~2.9 and ~6.1 for Cs^+, K^+ and Li^+, respectively. These ratios are in line with the hydration numbers of Li^+, K^+ and Cs^+ (Figure 3d). Thereby, the relatively large hydration number of cation (such as Li^+) corresponds to the high crossover rate of water via the CEM, resulting in a substantial increase in catholyte volume after electrolysis (Figure 3a).

It should be noted that the continuous electrolysis with CEMs in most of carbonate or bicarbonate electrolytes would lead to a dramatic decrease in anolyte concentration over electrolysis, which corresponds to a rapid drop in the anolyte conductivity (enhanced cell potentials in Figure S8), owing to the consumption of both cation species (transport to catholyte) and existing anion species (CO_2 degassing) in the anolyte over the course of electrolysis.[12] However, when using electrolytes that do not react with H^+, there may not be a reduced anolyte conductivity with a CEM. For instance, we even observed a decrease in cell potentials in CO_2 electrolysis in Li_2SO_4 electrolyte (Figure S9), which is due to that the H^+ generation at the anode/electrolyte interface could slowly transform the anolyte from Li_2SO_4 to H_2SO_4 over long-term electrolysis.

With the use of BPM, we found no obvious water crossover between the catholyte and the anolyte even after 5 h electrolysis at 200 mA/cm^2 (Figure S10), due to no obvious transportation of cation or anion species through the BPM. Based on all of the above findings, the water crossover for different ion-selective membranes can be summarized: (i) water could transport from catholyte to anolyte when transferring hydrated anions via an AEM (Figure 2d), in contrast, (ii) water would cross from anolyte to catholyte with transferring hydrated cations via a CEM (Figure 3d), and (iii) with the use of a BPM, there would be no obvious water crossover.

Effect of water crossover on liquid products analysis

When an AEM is used, a substantial water crossover from catholyte to anolyte via the AEM may significantly reduce the catholyte volume (Figure 2d). Thus, without considering the water crossover (*i.e.* variation in catholyte volume), the faradaic efficiency of liquid products could be overestimated (Equation 1). Based on Equation S16, we found the overestimation ratios for FE of liquid products gradually enhanced upon increasing CO_2/CO electrolysis time when transferring the three different anions, respectively (Figure

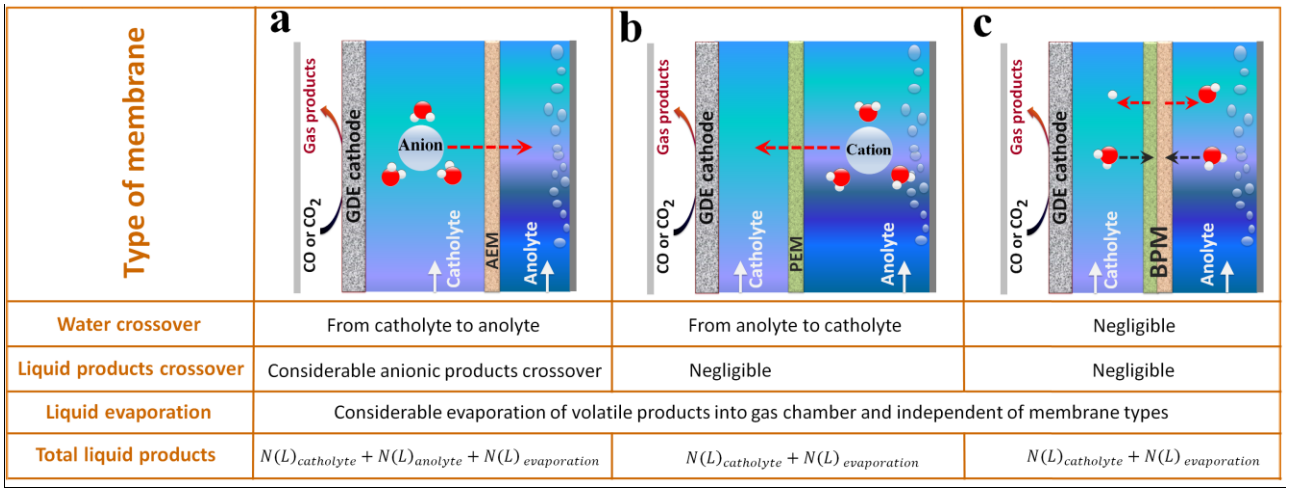

Figure 5. Schematic illustration of water crossover through different ion-selective membranes in three-compartment flow electrolyzers with benchmarking the analysis of their liquid products under consideration of water crossover: AEM (a), PEM (b) and BPM (c). The red and white balls correspond to O and H, respectively.

4a). This finding is ascribed to that the amount of water crossover is correlated with the total charge passed through the cathode if the charge-carrying anion species via the AEM is fixed (*i.e.* hydration number is fixed), as shown in Figure 2a. In addition, if the electrolysis is performed for 5 h (i.e. 7200 C), the overestimation ratios for FE of liquid products could be ~23%, ~15% and ~6% when only transferring HCO_3^-, CO_3^{2-} and OH^-, respectively (Figure 4a). The discrepancy in overestimation ratios of FE is due to that the amount of water crossover is linked to the hydration number of ions transferred via the AEM. Thereby, the liquid products could be significantly overestimated without consideration of water crossover, particularly when anionic species with large hydration number are utilized at elevated currents for long-term experiments.

In addition, the cathodic reactions also consume water with an AEM, which further reduces the catholyte volume (Scheme S1). It should be noted that this water consumption is linked to the catalytic selectivity (Equation S10). After considering the variation of the catholyte volume caused by both water crossover and this water consumption (Equation S17), the overestimation ratios for FE of liquid products could be ~25%, ~17% and ~8% (Figure S11) in this work, which is slightly larger than those for only consideration of water crossover in Figure 4a.

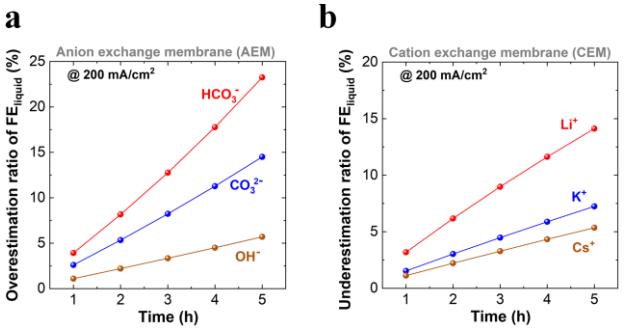

Figure 4. Overestimation and underestimation ratio of faradaic efficiencies of liquid products when using the AEM and the CEM, respectively (50 ml initial catholyte before electrolysis, active area of cathodic GDE is 2 cm^2).

With the use of a CEM, the water crossover from anolyte to catholyte occurs when transferring hydrated cations, correspondingly enhancing catholyte volume after electrolysis. Thereby, without the consideration of the water crossover, the faradaic efficiency of liquid products could be underestimated (Figure 4b). A BPM that avoids obvious water crossover would not significantly affect the faradaic efficiency calculations (by ignoring water evaporation) if the electrolysis time is not extremely long in lab-scale.

Suggested protocol of liquid product evaluation

For accurately evaluating catalytic selectivity of liquid products in flowing-catholyte electrolyzers with an AEM/CEM, we recommend the measurement of catholyte volume and anolyte volume after completion of electrolysis. Alternatively, if the charge-carrying ion species through the membranes is fixed, the volume of water crossover via membranes can be written as:

$$V_{H_2O\ Cross} \propto N_h \frac{Q_{tot}}{Fn_c} \cdot \frac{M_{H_2O}}{\rho} \quad (2)$$

where N_h and Q_{tot} are the hydration number of ions in water and the total charge passed through the membrane, respectively. F is the faradaic constant, n_c is the number of charges for each anion/cation, M_{H_2O} is the water molecular weight, and ρ is the density of water at ambient temperature and pressure. In addition, for an AEM the corrected hydration number of anions (Equation S18) should be used when considering water consumption induced by the cathodic reactions. Thus, with an AEM, the amount of liquid products dissolved in both catholyte and anolyte (using corrected volume of catholyte and anolyte) should be written as:

$$N(L)_{catholyte} = \mathrm{C_C} \times \left(\mathrm{V_C} - V_{H_2O\ Cross}\right) \quad (3)$$

$$N(L)_{anolyte} = \mathrm{C_A} \times \left(\mathrm{V_A} + V_{H_2O\ Cross}\right) \quad (4)$$

where, C_C and C_A are the detected concentration of liquid-phase products in catholyte and anolyte after electrolysis, respectively. V_C and V_A are the initial catholyte volume and initial anolyte volume before electrolysis, respectively.

Our previous work has demonstrated that both CEMs and BPMs are capable of inhibiting the crossover of anionic and neutral liquid products (Figure 5).[22] Thus, the amount of liquid products dissolved in electrolyte when using CEMs can be expressed as:

$$N(L)_{catholyte} = C_C \times \left(V_C + V_{H_2O\ Cross}\right) \quad (5)$$

Without an obvious variation in electrolyte volume for BPMs, the amount of liquid products dissolved in electrolyte is written as:

$$N(L)_{catholyte} = \mathrm{C_C} \times \mathrm{V_C} \quad (6)$$

It should be noted that liquid product evaporated into gas chamber ($N(L)_{evaporation}$) occurs with all membranes/separators. Thus,

$N(L)_{evaporation}$ should also be accounted for the total liquid products (Figure 5). Based on the proposed evaluation procedure (Figure 5), the reliable catalytic selectivity of the liquid products can be obtained for CO_2/CO electrolysis in three-compartment flow electrolyzers when using different ion-selective membranes.

Conclusions

In summary, our results show that water crossover when transferring hydrated ions as charge carriers via AEMs or CEMs in three-compartment electrolyzers could significantly change the electrolyte volume, which is closely correlated with the final evaluation of the catalytic selectivity for liquid products. Without the consideration of water crossover, the catalytic selectivity of liquid products could be overestimated with AEMs, and conversely, the catalytic selectivity of liquid products could be underestimated for CEMs. In this work, we proposed a rigorous protocol, which will enable us to achieve a more reliable quantification of liquid products for high-rate CO_2/CO electrolysis in three-compartment flow electrolyzers.

ASSOCIATED CONTENT

Supporting Information

Experimental procedures and additional data. This material is available free of charge via the Internet at http://pubs.acs.org.

AUTHOR INFORMATION

Corresponding Author

*Email: mingma@xjtu.edu.cn (M.M.)
*Email: brse@fysik.dtu.dk (B.S.)

Notes

The authors declare no competing financial interests.

ACKNOWLEDGMENT

This work is supported by National Natural Science Foundation of China (22179105) and “Young Talent Support Plan” of Xi’an Jiaotong University (awarded to M.M.). This work was also supported by ECOEthylene project from the Innovation Fund Denmark (Grant# 8057-00018B).

REFERENCES

(1) Seh, Z. W.; Kibsgaard, J.; Dickens, C. F.; Chorkendorff, I.; Nørskov, J. K.; Jaramillo, T. F. Combining Theory and Experiment in Electrocatalysis: Insights into Materials Design. *Science (80-.).* **2017**, *355* (6321), eaad4998. https://doi.org/10.1126/science.aad4998.

(2) Li, C. W.; Ciston, J.; Kanan, M. W. Electroreduction of Carbon Monoxide to Liquid Fuel on Oxide-Derived Nanocrystalline Copper. *Nature* **2014**, *508* (7497), 504–507. https://doi.org/10.1038/nature13249.

(3) Ma, M.; Djanashvili, K.; Smith, W. A. Controllable Hydrocarbon Formation from the Electrochemical Reduction of CO 2 over Cu Nanowire Arrays. *Angew. Chemie Int. Ed.* **2016**, *55* (23), 6680–6684. https://doi.org/10.1002/anie.201601282.

(4) Whipple, D. T.; Kenis, P. J. A. Prospects of CO2 Utilization via Direct Heterogeneous Electrochemical Reduction. *J. Phys. Chem. Lett.* **2010**, *1* (24), 3451–3458. https://doi.org/10.1021/jz1012627.

(5) De Luna, P.; Hahn, C.; Higgins, D.; Jaffer, S. A.; Jaramillo, T. F.; Sargent, E. H. What Would It Take for Renewably Powered Electrosynthesis to Displace Petrochemical Processes? *Science (80-.).* **2019**, *364* (6438), eaav3506. https://doi.org/10.1126/science.aav3506.

(6) Tan, X.; Yu, C.; Ren, Y.; Cui, S.; Li, W.; Qiu, J. Recent Advances in Innovative Strategies for the CO2electroreduction Reaction. *Energy Environ. Sci.* **2021**, *14* (2), 765–780. https://doi.org/10.1039/d0ee02981e.

(7) Hori, Y. Electrochemical CO2 Reduction on Metal Electrodes. In *Modern Aspects of Electrochemistry*; Vayenas, C. G., White, R. E., Gamboa-Aldeco, M. E., E., Ed.; Springer New York: New York, NY, 2004; Vol. 70, pp 89–189. https://doi.org/10.1007/978-0-387-49489-0_3.

(8) Ross, M. B.; Dinh, C. T.; Li, Y.; Kim, D.; De Luna, P.; Sargent, E. H.; Yang, P. Tunable Cu Enrichment Enables Designer Syngas Electrosynthesis from CO 2. *J. Am. Chem. Soc.* **2017**, *139* (27), 9359–9363. https://doi.org/10.1021/jacs.7b04892.

(9) Ma, M.; Liu, K.; Shen, J.; Kas, R.; Smith, W. A. In Situ Fabrication and Reactivation of Highly Selective and Stable Ag Catalysts for Electrochemical CO 2 Conversion. *ACS Energy Lett.* **2018**, *3* (6), 1301–1306. https://doi.org/10.1021/acsenergylett.8b00472.

(10) Birdja, Y. Y.; Pérez-Gallent, E.; Figueiredo, M. C.; Göttle, A. J.; Calle-Vallejo, F.; Koper, M. T. M. Advances and Challenges in Understanding the Electrocatalytic Conversion of Carbon Dioxide to Fuels. *Nat. Energy* **2019**, *4* (9), 732–745. https://doi.org/10.1038/s41560-019-0450-y.

(11) Verma, S.; Hamasaki, Y.; Kim, C.; Huang, W.; Lu, S.; Jhong, H.-R. M.; Gewirth, A. A.; Fujigaya, T.; Nakashima, N.; Kenis, P. J. A. Insights into the Low Overpotential Electroreduction of CO 2 to CO on a Supported Gold Catalyst in an Alkaline Flow Electrolyzer. *ACS Energy Lett.* **2018**, *3* (1), 193–198. https://doi.org/10.1021/acsenergylett.7b01096.

(12) Huang, J. E.; Li, F.; Ozden, A.; Sedighian Rasouli, A.; García de Arquer, F. P.; Liu, S.; Zhang, S.; Luo, M.; Wang, X.; Lum, Y.; Xu, Y.; Bertens, K.; Miao, R. K.; Dinh, C.-T.; Sinton, D.; Sargent, E. H. CO 2 Electrolysis to Multicarbon Products in Strong Acid. *Science (80-.).* **2021**, *372* (6546), 1074–1078. https://doi.org/10.1126/science.abg6582.

(13) Larrazábal, G. O.; Ma, M.; Seger, B. A Comprehensive Approach to Investigate CO 2 Reduction Electrocatalysts at High Current Densities. *Accounts Mater. Res.* **2021**, *2* (4), 220–229. https://doi.org/10.1021/accountsmr.1c00004.

(14) Burdyny, T.; Smith, W. A. CO 2 Reduction on Gas-Diffusion Electrodes and Why Catalytic Performance Must Be Assessed at Commercially-Relevant Conditions. *Energy Environ. Sci.* **2019**, *12* (5), 1442–1453. https://doi.org/10.1039/C8EE03134G.

(15) Weng, L.-C.; Bell, A. T.; Weber, A. Z. Modeling Gas-Diffusion Electrodes for CO 2 Reduction. *Phys. Chem. Chem. Phys.* **2018**, *20* (25), 16973–16984. https://doi.org/10.1039/C8CP01319E.

(16) Ma, M.; Clark, E. L.; Therkildsen, K. T.; Dalsgaard, S.; Chorkendorff, I.; Seger, B. Insights into the Carbon Balance for CO 2 Electroreduction on Cu Using Gas Diffusion Electrode Reactor Designs. *Energy Environ. Sci.* **2020**, *13* (3), 977–985. https://doi.org/10.1039/D0EE00047G.

(17) Zhang, G.; Zhao, Z.-J.; Cheng, D.; Li, H.; Yu, J.; Wang, Q.; Gao, H.; Guo, J.; Wang, H.; Ozin, G. A.; Wang, T.; Gong, J. Efficient CO2 Electroreduction on Facet-Selective Copper Films with High Conversion Rate. *Nat. Commun.* **2021**, *12* (1), 5745. https://doi.org/10.1038/s41467-021-26053-w.

(18) Zhang, X.; Wang, Y.-G.; Gu, M.; Wang, M.; Zhang, Z.; Pan, W.; Jiang, Z.; Zheng, H.; Lucero, M.; Wang, H.; Sterbinsky, G. E.; Ma, Q.; Wang, Y.-G.; Feng, Z.; Li, J.; Dai, H.; Liang, Y. Molecular Engineering of Dispersed Nickel Phthalocyanines on Carbon Nanotubes for Selective CO2 Reduction. *Nat. Energy* **2020**, *5* (9), 684–692. https://doi.org/10.1038/s41560-020-0667-9.

(19) Tan, Y. C.; Lee, K. B.; Song, H.; Oh, J. Modulating Local CO2 Concentration as a General Strategy for Enhancing C–C Coupling in CO2 Electroreduction. *Joule* **2020**, *4* (5), 1104–1120. https://doi.org/10.1016/j.joule.2020.03.013.

(20) Pan, F.; Yang, Y. Designing CO 2 Reduction Electrode Materials by Morphology and Interface Engineering. *Energy Environ. Sci.* **2020**, *13* (8), 2275–2309. https://doi.org/10.1039/D0EE00900H.

(21) Zhang, J.; Luo, W.; Züttel, A. Crossover of Liquid Products from Electrochemical CO2 Reduction through Gas Diffusion Electrode and Anion Exchange Membrane. *J. Catal.* **2020**, *385*, 140–145.

https://doi.org/10.1016/j.jcat.2020.03.013.

(22) Ma, M.; Kim, S.; Chorkendorff, I.; Seger, B. Role of Ion-Selective Membranes in the Carbon Balance for CO 2 Electroreduction via Gas Diffusion Electrode Reactor Designs. *Chem. Sci.* **2020**, *11* (33), 8854–8861. https://doi.org/10.1039/D0SC03047C.

(23) Israelachvili, J. N. Interactions Involving Polar Molecules. In *Intermolecular and Surface Forces*; Elsevier, 2011; pp 71–90. https://doi.org/10.1016/b978-0-12-375182-9.10004-1.

(24) Kameda, Y.; Sasaki, M.; Hino, S.; Amo, Y.; Usuki, T. Neutron Diffraction Study on the Hydration Structure of Carbonate Ion by Means of 12C/13C Isotopic Substitution Method. *Phys. B Condens. Matter* **2006**, *385–386*, 279–281. https://doi.org/10.1016/j.physb.2006.05.067.

(25) Leung, K.; Nielsen, I. M. B.; Kurtz, I. Ab Initio Molecular Dynamics Study of Carbon Dioxide and Bicarbonate Hydration and the Nucleophilic Attack of Hydroxide on CO2. *J. Phys. Chem. B* **2007**, *111* (17), 4453–4459. https://doi.org/10.1021/jp0684751.

(26) Kiss, A. M.; Myles, T. D.; Grew, K. N.; Peracchio, A. A.; Nelson, G. J.; Chiu, W. K. S. Carbonate and Bicarbonate Ion Transport in Alkaline Anion Exchange Membranes. *J. Electrochem. Soc.* **2013**, *160* (9), F994–F999. https://doi.org/10.1149/2.037309jes.

(27) Kopljar, D.; Inan, A.; Vindayer, P.; Wagner, N.; Klemm, E. Electrochemical Reduction of CO2 to Formate at High Current Density Using Gas Diffusion Electrodes. *J. Appl. Electrochem.* **2014**, *44* (10), 1107–1116. https://doi.org/10.1007/s10800-014-0731-x.

(28) Dufek, E. J.; Lister, T. E.; Stone, S. G.; McIlwain, M. E. Operation of a Pressurized System for Continuous Reduction of CO 2 . *J. Electrochem. Soc.* **2012**, *159* (9), F514–F517. https://doi.org/10.1149/2.011209jes.

(29) Reller, C.; Krause, R.; Volkova, E.; Schmid, B.; Neubauer, S.; Rucki, A.; Schuster, M.; Schmid, G. Selective Electroreduction of CO 2 toward Ethylene on Nano Dendritic Copper Catalysts at High Current Density. *Adv. Energy Mater.* **2017**, *7* (12), 1602114. https://doi.org/10.1002/aenm.201602114.

(30) Okada, T.; Satou, H.; Okuno, M.; Yuasa, M. Ion and Water Transport Characteristics of Perfluorosulfonated Ionomer Membranes with H + and Alkali Metal Cations. *J. Phys. Chem. B* **2002**, *106* (6), 1267–1273. https://doi.org/10.1021/jp013195l.